2,3,5,6-Tetraalkoxy-1,4-benzoquinones and structurally related tetraalkoxy benzene derivatives: synthesis, properties and solid state packing motifs

Erik M. D. Keegstra,[a] Bart-Hendrik Huisman,[a] Elizabeth M. Paardekooper,[a] Frans J. Hoogesteger,[a] Jan W. Zwikker,[a] Leonardus W. Jenneskens,*[,a] Huub Kooijman,[b] Arie Schouten,[b] Nora Veldman[b] and Anthony L. Spek[b]

[a] *Debye Institute, Department of Physical Organic Chemistry, Utrecht University, Padualaan 8, 3584 CH Utrecht, The Netherlands*
[b] *Bijvoet Center for Biomolecular Research, Crystal and Structural Chemistry, Utrecht University, Padualaan 8, 3584 CH Utrecht, The Netherlands*

A general synthesis of 2,3,5,6-tetraalkoxy-1,4-benzoquinones 1 from 1,2,4,5-tetraalkoxybenzenes 3 is reported. IR analysis (1a–e), the single crystal X-ray analysis of 2,3,5,6-tetramethoxy-1,4-benzoquinone 1a and semi-empirical calculations (AM1, 1a) show that the 1,4-benzoquinone skeleton possesses a merocyanine-type distortion. The solid state packing motifs of 1 are markedly affected by alkoxy chain length. For 1a, weak C–H · · · O interactions and reduction of unfavourable dipole–dipole interactions are important for intermolecular organization, whereas for 2,3,5,6-tetradecyloxy-1,4-benzoquinone [1e, wide angle X-ray diffraction (WAXD)] the close packing principle of the alkyl chains dominates. In both cases the results show that interplanar overlap is improved with respect to 1,4-benzoquinone 8. To deepen our insight into the effect of alkoxy chain length on solid state packing motifs, single crystal X-ray structures of methoxy and decyloxy derivatives of the structurally related compounds 1,4-diacetoxy-2,3,5,6-tetraalkoxybenzenes 2a and e, and 1,2,4,5-tetraalkoxybenzenes 3a and e were analysed. Compounds 1e, 2e and 3e, bearing decyloxy chains, possess board-like molecular structures which stack parallel along the *a*-axis as a result of alkyl chain interactions.

Since quinones possess multistage redox behaviour which can be modified by substitution,[1,2] considerable attention has been given to the preparation of derivatives for application in materials science. For example, they have been used in the development of artificial photosynthetic systems,[3] charge conducting materials,[4] electrode coatings,[5] coatings of metal surfaces[6] and optoelectronic display devices.[7] For many applications besides appropriate redox properties, intermolecular organization[8] leading to favourable π-overlap (quinone stacking) is an additional prerequisite.[9–11]

Although in the case of simple 1,4-benzoquinones available X-ray structural data show that they arrange themselves in planar ribbons or sheets due to intermolecular lateral hydrogen interactions between quinoid hydrogen and carbonyl oxygen atoms, in numerous cases favourable interplanar π-overlap is absent due to the fact that the parallel stacked quinones occupying successive planes are related by inversion and/or screw axis symmetry.

To improve the intermolecular organization we decided to introduce four alkoxy chains on the 1,4-benzoquinone skeleton, since there is ample evidence that this may improve intermolecular ordering between the constituents.[12] A literature survey revealed that 2,3,5,6-tetraalkoxy-1,4-benzoquinones **1** can be prepared by transetherfication of 2,3,5,6-tetramethoxy-1,4-benzoquinone with alkanols.[13] Unfortunately, this method is unsuited to the synthesis of derivatives containing aliphatic chains with $n > 5$; yields of only 6–22% are obtained after elaborate purification procedures.

Here we report a general synthesis for 2,3,5,6-tetraalkoxy-1,4-benzoquinones **1** from 1,2,4,5-tetraalkoxybenzenes. Insight into the physical properties of compounds **1** was obtained by cyclic voltammetry, differential scanning calorimetry (DSC) and semi-empirical quantum mechanical AM1 calculations. The influence of alkoxy chain length on the solid state organization was studied by comparing solid state packing motifs of **1a** and **e**. Although for **1a** a single crystal X-ray structure could be determined, no suitable single crystals of **1e** could be obtained. Nevertheless, an analysis of its wide angle X-ray diffraction (WAXD) pattern gave valuable information concerning its packing motif. To corroborate our analysis the effect of tetraalkoxy substitution on solid state packing motifs was further investigated for related compounds possessing a similar alkoxy chain substitution pattern, *i.e.* the methoxy and decyloxy derivatives of 1,4-diacetoxy-2,3,5,6-tetraalkoxy benzene (**2a** and **e**) and 1,2,4,5-tetraalkoxy benzenes (**3a** and **e**), respectively. Compounds **2a** and **e** are readily accessible from the corresponding 2,3,5,6-tetraalkoxy-1,4-benzoquinones **1a** and **e** *via* reductive acetylation and are potential monomers for novel rigid-rod polymers possessing a plate-like liquid crystalline phase (Scheme 1).[14]

Results and discussion

Synthesis

2,3,5,6-Tetraalkoxy-1,4-benzoquinones **1b–e** were prepared from 2,5-dihydroxy-1,4-benzoquinone **6** according to the procedure shown in Scheme 1. The 1,2,4,5-tetraalkoxybenzenes **3a–e** were obtained in high yield (83–96% after recrystallization) *via* a Williamson ether synthesis of 1,2,4,5-tetrahydroxybenzene **7** obtained *in situ* by hydrogenation of 2,5-dihydroxy-1,4-benzoquinone **6**.† Bromination of compounds **3a–e** in glacial acetic acid afforded the 1,4-dibromo-2,3,5,6-tetraalkoxybenzenes **4a–e** in 63–80% yield after recrystallization. Subsequently, compounds **4b–e** were converted into the 1,4-benzoquinones **1b–e** using the following one-pot procedure. Dilithiation of **4b–e** with butyllithium followed by boration with trimethyl borate

† It should be stipulated that hydrogenation and alkylation in DMF has considerable potential as a general method for reductive alkylation of quinones in a one-pot synthesis.

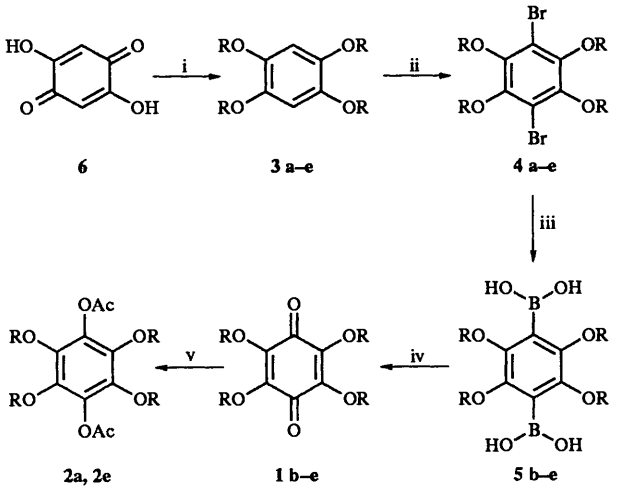

Scheme 1 **a** R = methoxy, **b** R = propoxy, **c** R = hexyloxy, **d** R = octyloxy, **e** R = decyloxy. *Reagents and conditions:* i, (a) PtO_2, H_2(g), DMF; (b) K_2CO_3, RBr; ii, Br_2, acetic acid; iii, (a) BuLi, diethyl ether; (b) $B(OCH_3)_3$; (c) H_2O, H^+; iv, (a) H_2O_2, H^+; (b) H_2O_2, K_2CO_3; v, Zn, AcCl, Ac_2O.

and hydrolysis of the borate ester groups gave the diboronic acid derivatives **5b–e**. Although compounds **5b–e** can be isolated and purified by crystallization (yield 30–61% with respect to **4b–e**), the crude products were directly oxidized using a two phase system (benzene–acidified hydrogen peroxide with a phase-transfer catalyst).‡ Initially a mixture of benzoquinone **1** and the related hydrobenzoquinone is obtained. Upon changing the pH to 8, the oxidation of the hydrobenzoquinones to benzoquinones **1** is completed. Purification by column chromatography gave compounds **1b–e** in 54–93% yield with respect to compounds **4b–e**. All products were characterized by ^1H and ^{13}C NMR, UV–VIS and IR spectroscopy and MS. Unfortunately, 2,3,5,6-tetramethoxy-1,4-benzoquinone **1a** could not be obtained following the above-mentioned procedure. This is attributed to the solubility of the diboronic acid **5a** in the aqueous hydroperoxide phase which apparently hampers its oxidation. As exemplified for the 2,3,5,6-tetraalkoxy-1,4-benzoquinones **1a** and **1e**, reductive acetylation[15] gave the related 1,4-diacetoxy-2,3,5,6-tetraalkoxybenzenes **2a** and **2e**, respectively, in excellent yield (80%).

Redox properties of compounds 1

To study the effect of alkoxy substitution on the redox properties of the 1,4-benzoquinone moiety, cyclic voltammograms were recorded for compounds **1a**,**c** and **e**, methoxy-1,4-benzoquinone **7** and the parent compound 1,4-benzoquinone **8** in acetonitrile. Since **1e** is insoluble in acetonitrile, both **1a** and **e** were measured using dichloromethane as solvent. For the conversion of these 1,4-benzoquinones to their radical anion (0/−1) and of the radical anion into the dianion (−1/−2), quasi-reversible and irreversible waves, respectively, were observed. As shown by the data in Table 1, alkoxy chain length has a minor influence on the redox properties. The moderate differences between the first reduction potentials [$\Delta E_{\frac{1}{2}}^{red}(0/-1)$] can be related to differences in electronic interaction at the cathode surface (40 mV between **1a** and **c** and 90 mV between **1a** and **e**). It is associated with an increase of the peak separation between the anodic and cathodic peak potential (ΔE_p) indicating a slower electron transfer process concomitant with increasing alkoxy chain length.[16] Comparing $E_{\frac{1}{2}}^{red}(0/-1)$ values in the series **1a**, **7** and **8** reveals that introduction of one methoxy group changes the $E_{\frac{1}{2}}^{red}(0/-1)$ of 1,4-benzoquinone by −0.09 V, while four methoxy groups changes $E_{\frac{1}{2}}^{red}(0/-1)$ by only −0.15 V. This is in marked contrast with the behaviour of the corresponding methyl substituted 1,4-benzoquinones where an average change of −0.09 V per methyl group was found.[17] As suggested in the literature,[18] an alkoxy substituent will affect the redox properties of the 1,4-benzoquinone unit *via* two separate opposing electronic interactions, *i.e.* a mesomeric electron donating effect and an inductive electron withdrawing effect. Although the mesomeric effect will dominate, it is only effective when the alkoxy substituent is co planar with the 1,4-benzoquinone π-system. In contrast, the inductive effect will always be operative regardless of the conformation of the alkoxy group due to its through-bond σ-character. Based on the moderate decrease of $E_{\frac{1}{2}}^{red}(0/1)$ in going from **1** to 1,4-benzoquinone **8** (−0.15 V), it is proposed that only two alkoxy substituents (presumably *para* related) are co planar with the 1,4-benzoquinone skeleton (*vide infra*).

Table 1 Reduction potentials of 2,3,5,6-tetraalkoxy-1,4-benzoquinones **1a**,**c** and **e**, methoxy-1,4-benzoquinone **7** and 1,4-benzoquinone **8** *vs.* ferrocene/ferrocinium

Compound	$E_{\frac{1}{2}}^{red}(0/-1)$/V	ΔE_p[c]/mV	$E_{\frac{1}{2}}^{red}(-1/-2)$[d]/V
1a[a]	−1.06	105	−2.1
1c[a]	−1.10	250	−2.2
1a[b]	−1.11	60	—[e]
1e[b]	−1.20	295	—[e]
7[a]	−1.00	150	−1.9
8[a]	−0.91	80	−2.0

[a] Solvent CH_3CN; reference electrode Ag/AgCl in CH_3CN (internal standard ferrocene/ferrocinium at 0.101 V). [b] Solvent CH_2Cl_2; reference electrode Ag/AgI in CH_3CN (internal standard ferrocene/ferrocinium at 0.866 V). [c] Peak separation between the anodic and cathodic peak potential (scan rate 100 mV s^{-1}). [d] Irreversible (ΔE_p > 300 mV). [e] Not detectable.

Table 2 Melting points (T_m), melting enthalpy (ΔH_m) and entropy (ΔS_m) of **1a–e**

Compound[a]	T_m[b]/°C	ΔH_m/kJ mol^{-1}	ΔS_m/J mol^{-1}
1a (n = 1)	127.0	29.4	74
1b (n = 3)	9.7	36.4	128
1c (n = 6)	−0.3	40.5	148
1d (n = 8)	14.2	58.3	203
1e (n = 10)	42.1	110.6	350

[a] n = number of carbon atoms per alkyl chain. [b] T_m onset of DSC transition.

Infrared analysis of compounds 1

In contrast to simple 1,4-benzoquinones, **1a–e** possess in both the solid state and in solution[19] a C=C stretch vibration at 1595 cm^{-1} with a remarkably strong intensity; it is more intense than the C=O stretch vibration at 1655 cm^{-1}. In fact, all methoxy substituted 1,4-benzoquinones display this phenomenon.[20] This signals the presence of considerable charge redistribution along the 1,4-benzoquinone perimeter and is indicative for a merocyanine-type (6π electron/5 centres) distortion of the 1,4-benzoquinone skeleton due to the mesomeric interaction between an alkoxy oxygen lone-pair and the 1,4-benzoquinone π-system (*vide infra*).[21]

Thermal properties of compounds 1

Differential scanning calorimetry (DSC) and polarization microscopy showed that compounds **1** possess only a melting peak; neither solid–solid phase transitions nor thermotropic liquid crystalline behaviour were discernible (Table 2). A survey of the melting points (T_m), the enthalpy (ΔH_m) and entropy (ΔS_m) change at T_m concomitant with alkoxy chain length

‡ ^1H NMR established the complete disappearance of **5b–e** under acid conditions, in contrast to neutral or basic conditions.

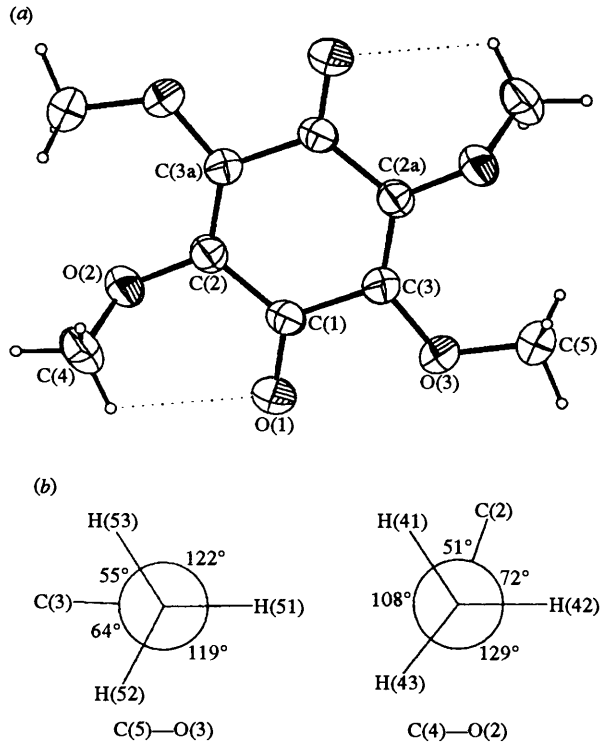

Fig. 1 Molecular structure of 2,3,5,6-tetramethoxy-1,4-benzoquinone **1a** showing (*a*) ORTEP drawing (50% probability level, intramolecular close C–H · · · O contact is represented by a dotted line), (*b*) Newman projection along C(5)–O(3) and Newman projection along C(4)–O(2)

indicates that T_m strongly decreases going from **1a** to **c** and increases from **1c** to **e**. This suggests that the 2,3,5,6-tetraalkoxy-1,4-benzoquinones containing short alkoxy substituents (**1a** and **b**) and those with longer alkoxy chains (**1c–e**) possess different solid-state structures.§ This can be rationalized by invoking that compounds **1** can be viewed as molecules consisting of two parts, *e.g.* a rigid benzoquinone unit and four flexible alkoxy chains. Thus, for **1a** and **b** intermolecular interactions between the 1,4-benzoquinone units are expected to dominate and will determine T_m as well as ΔH_m and ΔS_m.[24] In contrast, the observed ΔH_m and ΔS_m values in the case of **1c,d** and **e**, and the increase of T_m concomitant with increasing alkoxy chain length, indicate that van der Waals interactions between the flexible alkoxy chains will become increasingly important, while interactions between the 1,4-benzoquinone units will be reduced with respect to **1a–b** (Table 2).[25]

Structural characterization of compounds 1a and 1e

To establish to what extent the molecular structure of the 1,4-benzoquinone unit is affected by extensive methoxy substitution and to assess its effect on the solid state packing motif, the single crystal X-ray structure of **1a** was elucidated. Since DSC analysis suggested differences in the molecular packing in going from **1a–b** to **1c–e**, it was also desirable to resolve the single X-ray crystal structure of **1e** which is a solid at ambient temperature. Unfortunately, multifarious crystallization experiments only gave crystals unsuitable for single crystal X-ray analysis. Nevertheless, its powder WAXD pattern could be interpreted utilizing structural information obtained for compound **1a** and established principles for close packing of alkyl chains (*vide infra*).[11,26]

Molecular structure of tetramethoxy-1,4-benzoquinone 1a. The molecular structure of compound **1a** is presented in Fig. 1(*a*), and its general crystal data are listed in Table 3. Salient bond distances, valence angles and torsion angles are reported in Table 4. Compound **1a** possesses inversion symmetry and a nearly planar 1,4-benzoquinone unit. Two *para*-related methoxy substituents at C(3) and C(3a) are nearly coplanar with the 1,4-benzoquinone unit (torsion angle 3°) and the two methoxy groups at C(2) and C(2a) deviate from the plane defined by the 1,4-benzoquinone unit (torsion angle 66°). Apparently, the latter out-of-plane deviation is required to minimize unfavourable steric interactions. Note however, the short intramolecular distance between one of the methyl hydrogen atoms of the out-of-plane methoxy groups and the carbonyl oxygen [C(4)–H · · · O=C 2.54 Å with C(4)–H · · · O(1) 110.0°]. This close hydrogen contact equals the sum of the van der Waals radii minus 0.18 Å (isotropic van der Waals radii; C 1.75, H 1.20, O 1.52 Å[27]). Newman projections along C(4)–O(2) and C(5)–O(3) reveal that torsion angles along C(4)–O(2) deviate from multiples of 60° [Fig. 1(*b*)].

In line with the data derived from cyclic voltammetry and IR spectroscopy, the 1,4-benzoquinone skeleton of compound **1a** possesses a distorted structure reminiscent of merocyanine-type structures,[28] *viz.* bond equalization occurs along the two discernible 6π-electron/5 centres subunits [O(1)–C(1)–C(2)–C(3a)–O(3a)]. These subunits are connected by substantially elongated single sp^2–sp^2 carbon–carbon bonds [C(1)–C(3)]; the difference in length between C(1)–C(2) and C(1)–C(3) is 0.027 Å. A substantial contraction of the C(3)–O(3) bond [1.339(2) Å] and a deviation of the valence angle O(3)–C(3)–C(2a) (130.0°) for the in-plane methoxy substituents from the reference value 120.0° is observed. Nevertheless, the sum of valence angles (Σ) around carbon atom C(3) is 360.0° which indicates that considerable rehybridization has taken place around these carbon atoms [σ-framework hybridization (sp^n) for C(3): C(3)–C(2a), n = 1.04; C(3)–O(3), n = 2.28 and C(1)–C(3), n = 3.86].[29] In contrast for C(2) containing the out-of-plane methoxy group, the deviations are considerably smaller [Σ = 359.8° σ-framework hybridization sp^n around C(2), respectively: O(2)–C(2), n = 2.10; C(2)–C(3a), n = 1.62 and C(1)–C(2), n = 2.40]. Analogous structural distortions have been reported for 1,4-benzoquinone derivatives containing amine substituents.[1,30] Both experimental and theoretical evidence revealed that for the latter compounds the merocyanine-type distortion is a consequence of n/π and σ interactions between the amine lone pair and the α,β-unsaturated ketone fragments of the benzoquinone unit.[31] AM1 calculations on **1a** satisfactorily reproduce the X-ray results indicating that the found distortion of the benzoquinone skeleton is due to electronic interactions between the alkoxy substituents and the quinone moiety (Table 4).¶ Interestingly, the calculations indicate that **1a** can be described by the 'molecule in molecule approach',[31] *i.e.* **1a** consists of two head-to-tail linked 2,3-dimethoxyacrolein units.[21]

Solid state packing motif of compound 1a. The crystal structure of **1a** has the space group symmetry $P2_1/c$ and contains two molecules per unit cell. The crystal lattice in the [1 0 1] and [1 0 0] direction is shown in Fig. 2(*b*) and (*c*). Note the one-dimensional parallel stacking of the 1,4-benzoquinone units along the *a*-axis with a typical interplanar distance of 3.48 Å between two successive least-squares planes defined by the 1,4-benzoquinone units. The length of the *a*-axis (4.00 Å) together with a tilt angle of 29.5° between the normal on the 1,4-benzoquinone plane and the stacking axis is indicative of a close packed one-dimensional columnar structure enabling π-overlap between adjacent molecules. To reduce unfavourable dipole–

§ Recently, a similar interpretation was reported for tetrakis(alkylsulfanyl)tetrathiafulvalenes[22] and 1- or 2-alkylnaphthalenes[23] for which an analogous dependence of T_m upon the length of alkyl chains was found.

¶ With MNDO[32] or PM3[33] all methoxy substituents deviate from the plane of the 1,4-benzoquinone skeleton in the optimized structure of **1a**. This can be attributed to their tendency to overestimate steric crowding.[34]

Table 3 Crystallographic data for **1a**, **2a**, **2e** and **3e**

Complex	**1a**	**2a**	**2e**	**3e**
Crystal data				
Formula	$C_{10}H_{12}O_6$	$C_{14}H_{18}O_8$	$C_{50}H_{90}O_8$	$C_{46}H_{86}O_4$
Molecular mass	228.20	314.29	819.26	703.19
Crystal system	Monoclinic	Monoclinic	Triclinic	Triclinic
Space group	$P2_1/c$ (No. 14)	$P2_1/a$ (No. 14)	$P\bar{1}$ (No. 2)	$P\bar{1}$ (No. 2)
a/Å	4.001(1)	8.0060(3)	5.4788(4)	4.696(5)
b/Å	7.730 0(8)	11.5147(5)	11.3655(8)	15.371(6)
c/Å	16.952(2)	9.2512(4)	20.977(2)	17.075(15)
α/°	90	90	95.92(1)	72.47(6)
β/°	99.54(2)	112.793(3)	93.31(1)	85.44(8)
γ/°	90	90	97.59(1)	81.55(7)
V/Å^3	517.0(2)	786.24(6)	1284.5(2)	1161.7(18)
D_c/g cm^{-3}	1.466	1.327	1.059	1.005
Z	2	2	1	1
F(000)	240	332	454	394
μ/cm^{-1}	1.2	1.0	0.6	4.4
Crystal size/mm	0.10 × 0.12 × 0.75	0.3 × 0.7 × 0.7	0.2 × 0.2 × 0.6	0.10 × 0.10 × 0.75
Data collection				
T/K	298	298	298	295
θ_{min}, θ_{max}/°	2.4, 27.5	1.8, 27.5	1.0, 27.5	2.7, 69.0
SET4 θ_{min}, θ_{max}/°	9.8, 15.5	11.0, 21.0	9.9, 13.9	14.8, 27.0
λ/Å	0.710 73 (Mo-Kα) (graphite mon.)	0.710 73 (Mo-Kα) (Zr filter)	0.710 73 (Mo-Kα) (graphite mon.)	1.541 84 (Cu-Kα) (Ni filter)
Scan type	ω–2θ	ω–2θ	ω–2θ	ω–2θ
Δw/°	1.06 + 0.35 tan θ	0.94 + 0.35 tan θ	0.61 + 0.35 tan θ	1.38 + 0.14 tan θ
Hor., ver. aperture/mm	4.58, 4.00	3.00, 4.00	3.00, 4.00	4.12, 6.00
X-Ray exposure time/h	20	51	30	45
Linear decay (%)	< 1	1	2	< 1
Reference reflections	2 $\bar{2}$ 3, 1 $\bar{2}$ $\bar{8}$, $\bar{1}$ 3 $\bar{1}$	2 $\bar{2}$ 0, 2 2 $\bar{3}$, $\bar{1}$ 2 2	$\bar{2}$ 0 $\bar{3}$, 1 2 $\bar{4}$, 1 3 2	2 1 $\bar{4}$, 1 2 3, 1 $\bar{6}$ $\bar{2}$
Data set (h,k,l)	−5:5, −10:0, −22:22	−10:10, 0:14, −12:12	−7:7, −14:14, −27:27	0:5, −17:17, −20:19
Total data	2922	3519	7565	4374
Total unique data	1192 (R_{int} = 0.051)	1805 (R_{int} = 0.023)	5855 (R_{int} = 0.015)	3850 (R_{int} = 0.06)
Observed data	[No. obs. crit. applied]	1255 [$I > 2.5\sigma(I)$]	3676 [$I > 2.5\sigma(I)$]	1812 [$I > 2.5\sigma(I)$]
Absorption corr. range	—	—	—	0.55, 1.55 (DIFABS)
Refinement				
No. of refined params.	97	111	443	237
Final R[a]	0.043 [739 $I > 2\sigma(I)$]	0.043	0.047	0.097
Final $wR2$[b]	0.126	—	—	—
Final R_w[c]	—	0.037	0.039	0.137
Goodness of fit	1.02	0.36	0.44	0.84
w^{-1}[d]	$\sigma^2(F^2) + (0.0673P)^2$	$\sigma^2(F)$	$\sigma^2(F)$	$\sigma^2(F) + 0.0093\,F^2$
$(\Delta/\sigma)_{av}$, $(\Delta/\sigma)_{max}$	0.004, 0.064	0.035, 0.629	0.009, 0.066	0.019, 0.077
Min. and max. residual density/e Å^{-3}	−0.19, 0.21	−0.16, 0.21	−0.21, 0.19	−0.33, 0.43

[a] $R = \Sigma||F_o| - |F_c||/\Sigma|F_o|$. [b] $wR^2 = \{\Sigma[w(F_o^2 - F_c^2)^2]/\Sigma[w(F_o^2)^2]\}^{\frac{1}{2}}$. [c] $R_w = \{\Sigma[w(|F_o| - |F_c|)^2]/\Sigma[w(F_o^2)]\}^{\frac{1}{2}}$. [d] $P = [\mathrm{Max}(F_o^2, 0) + 2F_c^2]/3$.

dipole interactions between merocyanine-type subunit perimeters [O(1)–C(1)–C(2)–C(3a)–O(3a)] of adjacent molecules, they are positioned anti-parallel [Fig. 2(*b*)]. A similar minimalization of intermolecular merocyanine-type dipole–dipole interactions was found for methoxy-1,4-benzoquinone **7**[21] and 2,5-dialkoxy-1,4-benzoquinones.[35] In the *b*-direction the one-dimensional columnar arrangement is repeated by an orthogonal displacement, while in the *c*-direction the columns are related by glide plane symmetry [Fig. 2(*c*)]. In the direction [1 0 1] a ribbon-type pattern is discernible between coplanar adjacent molecules due to weak C–H···O interactions between in-plane methyl hydrogen atoms H(51) and H(51a), and the carbonyl oxygens O(1) and O(1a), respectively (Fig. 3). The H···O distance 2.59 Å equals the sum of van der Waals radii minus 0.13 Å and the C–H bond lies in the plane defined by the oxygen lone pairs; a C–H···O angle of 156.2° and a H···O=C angle of 125.7° which are almost ideal (Table 5). In addition, weaker C–H···O contacts exist between the in-plane methyl hydrogen atoms H(51) and H(51a), and the in-plane methoxy oxygens O(3) and O(3a), respectively. The C–H bond points between the lone pairs of the oxygen [the H···O distance 2.64 Å equals the sum of van der Waals radii minus 0.08 Å and C(5)–H···O, H···O–C(3) and H···O–C(5) angles of 142.1, 124.0 and 112.2°, respectively, Table 5]. These short contacts can be classified as bifurcated.[36] The directionality of the ether hydrogen bond is less pronounced than that of the carbonyl oxygen. Fig. 3 shows the close hydrogen contacts between two adjacent molecules in a ribbon. They are related by an inversion centre with the in-plane C–H bonds pointing towards the lone pairs of the carbonyl oxygens and in between the lone pairs of the in-plane methoxy oxygens giving infinite nearly planar ribbons.

Although the directional properties of the C–H···O interactions between quinoid hydrogens and carbonyl oxygens have been recognized,[8,37] weak hydrogen bond interactions between methyl hydrogens and quinoid carbonyl oxygens are rare. Recently, we found another example in the case of methoxy-1,4-benzoquinone **7**.[21] It should be stipulated that the directionality of the bifurcated weak methyl hydrogen contacts in **1a** and **7** possess a strong resemblance. The effect of C–H···O interactions on the packing motif of **1a** is further supported by a comparison of its density (**1a**, 1.47 g cm^3) with those of structurally related compounds **2a** (1.33 g cm^{-3}) and **3a** (1.31 g cm^{-3}). In the latter two compounds C–H···O interactions are absent (*vide infra*).

The crystal structure of **1a** consists of closely packed parallel ribbons giving a two-dimensional layer [Fig. 2(*b*)].[24,38] Obviously, van der Waals interactions between the out-of-plane

Table 4 Selected structural features from the single crystal X-ray structure of 2,3,5,6-tetramethoxy-1,4-benzoquinone **1a**. AM1 results between square brackets[a]

Bond lengths (Å)		
C(1)–C(2)	1.473(2)	[1.475]
C(1)–C(3)	1.500(2)	[1.500]
C(2)–C(3a)[b]	1.339(2)	[1.359]
C(1)–O(1)	1.211(2)	[1.232]
C(2)–O(2)	1.369(2)	[1.386]
C(3)–O(3)	1.339(2)	[1.364]
C(4)–O(2)	1.442(3)	[1.431]
C(5)–O(3)	1.428(3)	[1.427]
Bond angles (°)		
O(2)–C(2)–C(3a)[b]	123.38(15)	[120.85]
O(2)–C(2)–C(1)	116.25(14)	[116.71]
C(1)–C(2)–C(3a)[b]	120.15(14)	[122.17]
C(2)–C(1)–C(3)	119.59(14)	[115.39]
O(1)–C(1)–C(2)	120.33(15)	[123.17]
O(1)–C(1)–C(3)	120.05(15)	[121.44]
C(1)–C(3)–C(2a)[b]	120.23(15)	[121.64]
O(3)–C(3)–C(2a)[b]	130.03(16)	[128.02]
O(3)–C(3)–C(1)	109.74(14)	[110.33]
C(3)–O(3)–C(5)	122.12(16)	[118.52]
C(2)–O(2)–C(4)	115.40(16)	[114.53]
Torsion angles (°)		
C(3a)[b]–C(2)–O(2)–C(4)	−114.3(2)	[−115.82]
C(2a)[b]–C(3)–O(3)–C(5)	−2.8(3)	[−1.04]

[a] See Experimental section. [b] Atoms generated by symmetry operation $1-x, 1-y, -z$.

methyl groups and dipole–dipole interactions between the 1,4-benzoquinone units in the planes are of importance in the parallel packing motif which is complemented by crossed stacking of the layers (not shown). As implicated by their H···O distances (2.58 Å) and their C–H···O (173.0°) and H···O=C (153.2°) angles, C–H···O=C hydrogen contacts are also present between the crossed layers, albeit with less pronounced directionality.

The solid state structure of tetradecyloxy-1,4-benzoquinone 1e. Compound **1e** can be envisaged to consist of two different parts, *i.e.* a rigid 2,3,5,6-tetraoxy-1,4-benzoquinone core and four flexible decyl chains. Hence, it is expected that the different parts will tend to assemble in separated microdomains.[11] It is well documented that hydrocarbon chains prefer a two-dimensional layered packing of plane-zigzag (antiperiplanar) chains with their axes running parallel.[24] Under this assumption, it is expected that in the case of **1e** the 1,4-benzoquinone units will stack in either one-dimensional ribbons or two-dimensional layers separated by close packed alkyl chains.[11,36] In its powder wide angle X-ray diffractogram the [0 0 1] and higher order reflections are clearly visible yielding a $1/c^*$ value of 30.97 Å (c^* = reciprocal c axis) which corresponds remarkably well with the extended molecular length of **1e** derived from a CPK (Corey–Pauling–Koltun) space-filling model with antiperiplanar alkoxy chains (31.5 Å). This suggests that in the solid state, compound **1e** will be organized in two-dimensional layers, hence, the alkoxy chain axes have to be nearly parallel with c^* and the reciprocal unit cell angles α^* and β^* should possess values close to 90°. Under these conditions we were able to assign all [h k l] reflections. A comparison of experimental $4-\theta$ values, the corresponding diffraction spacings and calculated $4-\theta$ values are presented in Table 6; an excellent agreement is found. The matching unit cell parameters are $a = 4.80$, $b = 8.16$, $c = 31.22$ Å, $\alpha = 96.9$, $\beta = 90.2$ and $\gamma = 105.8°$. Additional insight into the solid state structure of **1e** was derived from its solid state IR spectrum and examination of its CPK model. As discussed, the presence of a strong intensity C=C stretch vibration for **1a–e** provides evidence that **1e** possesses a merocyanine-type distortion of its

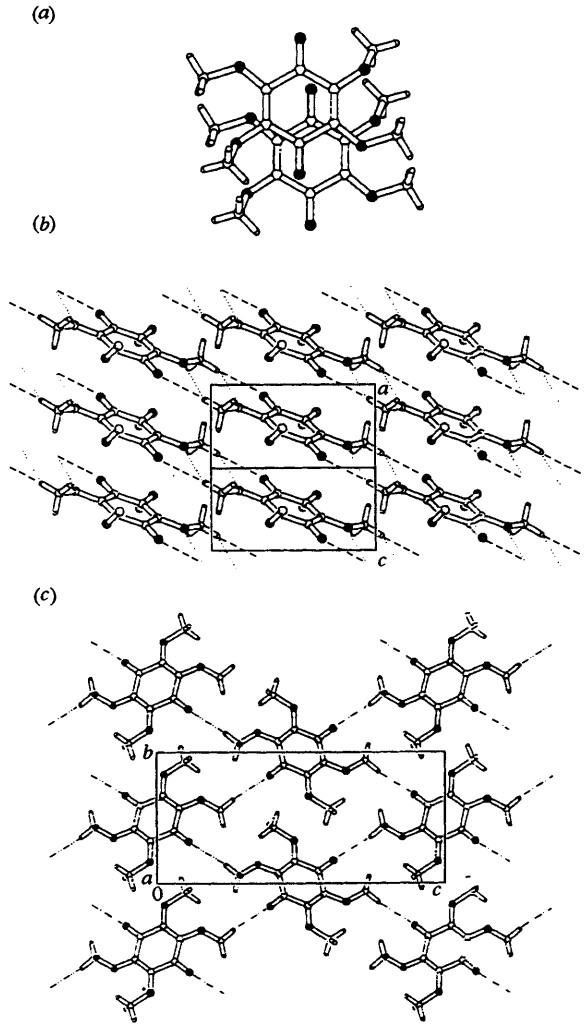

Fig. 2 Packing structure of compound **1a** (intermolecular close C–H···O contacts are represented by dashed lines) showing (*a*) plane-to-plane intermolecular overlap in the *a*-direction viewed perpendicular to the 1,4-benzoquinone plane, (*b*) [1 0 1] projection (hydrogen atoms at C(4) are omitted for clarity), (*c*) [1 0 0] projection

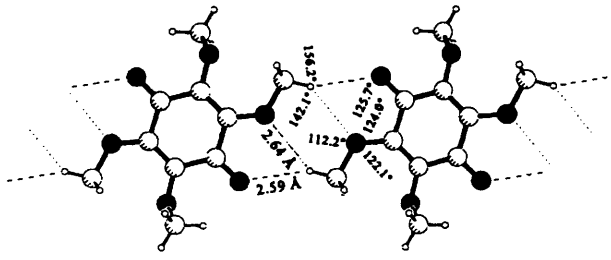

Fig. 3 Ribbon-type structure of **1a** viewed perpendicular to the 1,4-benzoquinone plane; lateral C–H···O contacts are represented by dashed lines

1,4-benzoquinone skeleton due to mesomeric interactions with two *para*-related alkoxy substituents. In order to obtain a molecular length of 31.5 Å, the alkoxy chains have to align longitudinally, presumably *via* introduction of a gauche kink in the in-plane alkoxy groups near the 1,4-benzoquinone moiety. Since $1/c^*$ is almost parallel with the alkyl chain axes, the *ab* crystal plane coincides with the a_0b_0 plane of the alkyl chain subcell determined by the position of the methylene groups.[24] Its area (37.7 Å^2) is close to twice the area of the a_0b_0 plane of a triclinic subcell (18.73 Å^2).[24] This analysis provides compelling evidence that substitution of 1,4-benzoquinone with alkoxy groups leads to self-organization of the 1,4-benzoquinone moiety into a columnar arrangement with improved interplanar π-type interactions between the 1,4-benzoquinones

Table 5 Lateral intermolecular hydrogen contacts in and between ribbon motifs of 2,3,5,6-tetramethoxy-1,4-benzoquinone **1a** and 1,4-benzoquinone **8**[55]

Compound	H···O contact	$d_{(H\cdots O)}$/Å	∠(C=O···H)/°	∠(C–O···H)/°	∠(C–H···O)/°
1a	Methyl H···O=C[a]	2.59	125.7		156.2 142.1 C(5)
	Methyl H···O–C[a]	2.64		112.2 C(5) 124.0 C(3)	
8	Quinoid H···O=C[a]	2.38	133.1		166.4
	Quinoid H···O=C[b]	2.30	148.4		161.3

[a] In the plane of the ribbon. [b] Between ribbons (see Fig. 3).

Table 6 Wide angle powder X-ray diffraction (WAXD) data of 2,3,5,6-tetradecyloxy-1,4-benzoquinone **1e**

h k l reflection	Calc. 4 – θ/°	Exp. 4 – θ/°	Diffraction spacing/Å
0 0 1	5.7	5.7	30.97
0 0 3	17.1	17.1	10.32
0 1 0/0 1 −1	22.7	22.7	7.70
0 1 1/0 1 −2	24.1	24.1	7.34
0 1 2/0 1 −3	26.7	26.7	6.63
1 0 0	38.4	38.4	4.62
1 −1 0	38.9	38.9	4.56
1 0 1	39.5	39.5	4.49
1 0 −2	39.7	39.7	4.47
1 −1 −2	40.2	40.2	4.42
1 0 2	41.0	41.0	4.33
1 −1 −3	42.0	42.0	4.23
1 −1 3	43.2	43.1	4.12
1 −1 −4	44.5	44.5	3.99

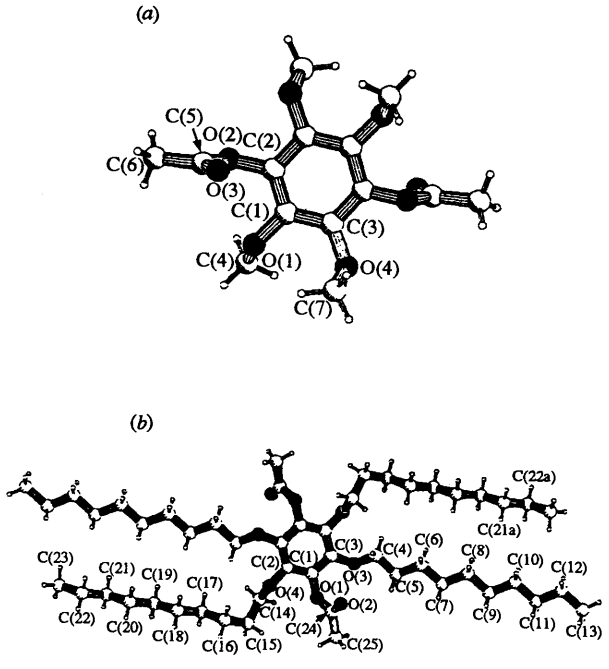

Fig. 4 Single crystal X-ray structures of **2a** (*a*) and **2e** (*b*)

occupying successive planes. In the case of **1a**, the observed close columnar stacking (length of *a*-axis is 4.0 Å) is primarily due to numerous weak C–H···O contacts and the minimalization of dipole–dipole interactions. For **1e** the solid state packing is primarily determined by the close packing principle of the alkyl chains.

Since no suitable single crystals of **1e** were available, the X-ray structures of structurally related compounds **2a** and **e**, and **3a** and **e**, possessing a similar substitution pattern, were determined to deepen our insight into the self-organization effect by tetraalkoxy substitution.

Table 7 Selected structural features of the single X-ray structure of **2a**

Bond lengths (Å)	
O(1)–C(1)	1.373(2)
O(1)–C(4)	1.421(3)
O(2)–C(2)	1.394(2)
O(2)–C(5)	1.362(2)
O(3)–C(5)	1.188(3)
O(4)–C(3)	1.376(2)
O(4)–C(7)	1.432(3)
C(1)–C(2)	1.385(2)
C(1)–C(3)	1.389(2)
C(2)–C(3a)	1.386(3)
C(5)–C(6)	1.485(3)
Bond angles (°)	
C(1)–O(1)–C(4)	114.34(16)
C(2)–O(2)–C(5)	116.05(14)
C(3)–O(4)–C(7)	113.93(16)
O(1)–C(1)–C(2)	119.21(16)
O(1)–C(1)–C(3)	121.19(16)
C(2)–C(1)–C(3)	119.58(17)
O(2)–C(2)–C(1)	118.61(16)
O(2)–C(2)–C(3a)	119.56(15)
O(4)–C(3)–C(1)	121.94(16)
O(4)–C(3)–C(2a)	119.36(16)
C(1)–C(3)–C(2a)	118.67(16)
O(2)–C(5)–C(6)	110.86(17)
O(3)–C(5)–C(6)	127.11(19)
Torsion angles (°)	
C(3)–C(1)–C(2)–C(3a)	0.1(3)
O(1)–C(1)–C(3)–O(4)	2.8(3)
O(1)–C(1)–C(2)–O(2)	−4.5(3)
O(2)–C(2)–C(3a)–O(4a)	4.9(3)
C(3)–C(1)–O(1)–C(4)	−83.0(2)
C(1)–C(2)–O(2)–C(5)	79.1(2)
C(1)–C(3)–O(4)–C(7)	−69.7(2)
C(2)–O(2)–C(5)–C(6)	−172.16(16)

Structural characterization of 1,4-diacetoxytetraalkoxybenzenes 2a and 2e

In Fig. 4 the single crystal X-ray structures of **2a** and **e** are presented (*cf.* Table 3 for general crystal data). Relevant bond distances, valence angles and torsion angles are listed in Tables 7 and 8. In these overcrowded centrosymmetric molecules the substituents are positioned above and below the planar central benzene ring [torsion angles C(3)–C(1)–O(1)–C(4) = −83.0° (**2a**), C(1)–C(2)–O(2)–C(5) = 79.1° (**2a**), C(1)–C(3)–O(4)–C(7) = 69.7° (**2a**), C(2)–C(1)–O(1)–C(24) = −108.2° (**2e**), C(1)–C(2)–O(4)–C(14) = −71.3° (**2e**), C(1)–C(3)–O(3)–C(4) = −134.2° (**2e**)].

Compound **2a** crystallizes in the space group $P2_1/a$, $Z = 2$ leading to a herringbone-like packing motif which coincides with the *ab* plane (Fig. 5). Along the *c*-axis the layers are related *via* a monoclinic displacement. Due to the bulky substituents and the presence of glide plane symmetry, the centre-to-centre distance between successive benzene rings is substantial (*a*-axis 8.01 Å, tilt angle between the normal on the benzene plane and the *a*-axis 40.9° and perpendicular distance between successive

Table 8 Selected structural features of the single X-ray structure of **2e**

Bond lengths (Å)	
O(1)–C(1)	1.396(2)
O(1)–C(24)	1.362(2)
O(2)–C(24)	1.190(3)
O(3)–C(3)	1.370(2)
O(3)–C(4)	1.441(2)
O(4)–C(2)	1.373(2)
O(4)–C(14)	1.459(2)
C(1)–C(2)	1.395(2)
C(1)–C(3)	1.383(2)
C(2)–C(3a)	1.393(2)
C(24)–C(25)	1.489(4)
C(4)–C(5)	1.499(3)
C(5)–C(6)	1.511(4)
C(14)–C(15)	1.500(3)
C(15)–C(16)	1.522(3)
C(16)–C(17)	1.518(3)
Bond angles (°)	
C(1)–O(1)–C(24)	118.18(14)
C(3)–O(3)–C(4)	117.61(13)
C(2)–O(4)–C(14)	115.85(13)
O(1)–C(1)–C(2)	117.59(14)
O(1)–C(1)–C(3)	119.32(15)
C(2)–C(1)–C(3)	123.03(16)
O(3)–C(3)–C(1)	116.26(15)
O(3)–C(3)–C(2a)	124.62(15)
O(4)–C(2)–C(1)	120.81(15)
O(4)–C(2)–C(3a)	120.94(15)
C(1)–C(3)–C(2a)	118.98(15)
O(1)–C(24)–C(25)	109.0(2)
O(2)–C(24)–C(25)	127.5(2)
O(3)–C(4)–C(5)	108.29(16)
C(4)–C(5)–C(6)	112.34(18)
O(4)–C(14)–C(15)	107.79(15)
C(14)–C(15)–C(16)	115.07(17)
C(15)–C(16)–C(17)	114.11(18)
Torsion angles (°)	
C(3)–C(1)–C(2)–C(3a)	0.9(3)
O(1)–C(1)–C(2)–O(4)	9.7(2)
O(1)–C(1)–C(3)–O(3)	0.3(2)
O(4)–C(2)–C(3a)–O(3a)	−2.2(3)
C(1)–C(3)–O(3)–C(4)	−134.20(17)
C(3)–O(3)–C(4)–C(5)	153.67(16)
O(3)–C(4)–C(5)–C(6)	169.33(19)
C(1)–C(2)–O(4)–C(14)	−71.3(2)
C(2)–O(4)–C(14)–C(15)	163.12(15)
O(4)–C(14)–C(15)–C(16)	67.1(2)
C(14)–C(15)–C(16)–C(17)	72.5(2)
C(1)–O(1)–C(24)–C(25)	−178.10(17)

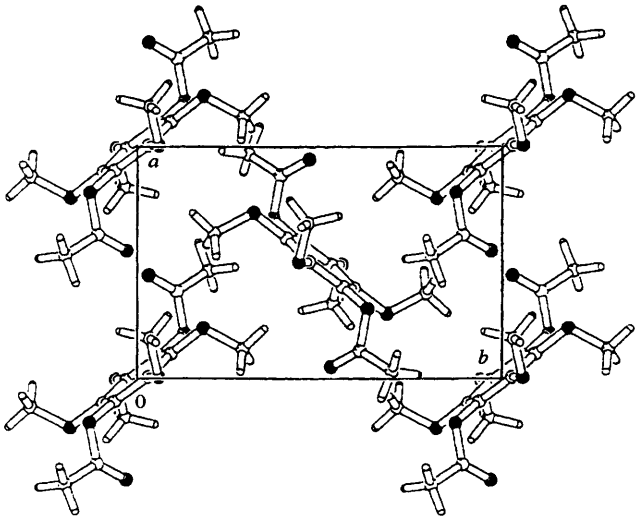

Fig. 5 Packing structure of **2a**; [0 0 1] projection

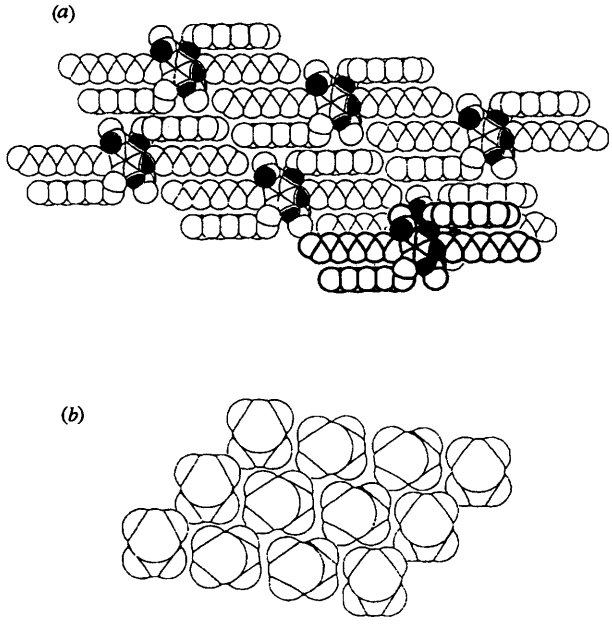

Fig. 6 CPK drawings of the alkyl chain packing of compound **2e** showing (*a*) top view (hydrogen atoms are omitted for clarity, one molecule in an adjacent layer is depicted bold), (*b*) cross-section showing C(10), C(9), C(22a) and C(21a) [for atom labels see Fig. 4(*b*)]

benzene rings 6.0 Å). Hence, favourable π-overlap between successive benzene rings is hampered. Compound **2e** [space group $P\bar{1}$ ($Z = 1$) containing four decyloxy chains] possesses a board-like structure. Fig. 6(*a*) reveals that the intermolecular ordering of the benzene moieties is markedly affected by the close packing principle of the decyl chains. As expected they possess a nearly extended antiperiplanar conformation. Note the presence of gauche kinks in two *para*-related alkoxy chains leading to efficient close packing of the alkoxy chains in an rectangular arrangement (Fig. 6). A cross-section through the alkoxy chain packing [C(10), C(9), C(22a) and C(21a) shown, see Fig. 4] is given; typical oblique and rectangular packing motives are found.[24] The benzene rings are stacked by translation in the direction of the *a*-axis coming out of the plane of the drawing. Concurrently, a reduction of the centre-to-centre distance to 5.47 Å between the benzene moieties is discernible (tilt angle 35.7°). However, due to the bulky acetoxy substituents, the perpendicular distance between two successive benzene rings (4.5 Å) still deviates from the optimal value (3.4 Å). Remarkable is the absence of a two-dimensional layered packing of the alkyl chains characteristic for paraffins; *viz.* no plane perpendicular to the alkyl chain axes through their end groups can be drawn separating layers of molecules.[25] Instead the alkyl chains interlock like bricks in a wall in both the *b* and *c* direction.

The differences found between the solid state structures of **2a** and **e** demonstrate that long alkoxy substituents effectively influence intermolecular organization, *i.e.* improved self-organization with respect to possible π-overlap between benzene moieties occupying successive planes.

Structural characterization of tetraalkoxybenzenes 3a and 3e

The single crystal X-ray structure of 1,2,4,5-tetramethoxybenzene **3a** has been reported previously.[39] Compound **3a** crystallizes in a tetragonal lattice (space group $P4_2/n$ with four molecules per unit cell) with axial symmetry around the *c*-axis and possesses a nearly planar centrosymmetrical molecular structure. The aromatic rings stack parallel in the *c* direction with a tilt angle (57.4°) between the stacking axes and the plane defined by the benzene moiety. The centre-to-centre distance is 5.04 Å and the perpendicular distance between adjacent benzene

Table 9 Selected structural features of the single X-ray structure of **3e**

Bond lengths (Å)	
O(1)–C(2)	1.362(6)
O(1)–C(4)	1.421(6)
O(2)–C(3)	1.375(7)
O(2)–C(14)	1.427(7)
C(1)–C(2)	1.401(9)
C(1)–C(3a)	1.402(7)
C(2)–C(3)	1.371(8)
C(4)–C(5)	1.526(7)
C(5)–C(6)	1.497(8)
C(6)–C(7)	1.525(8)
C(7)–C(8)	1.492(8)
C(14)–C(15)	1.485(9)
C(15)–C(16)	1.483(9)
C(16)–C(17)	1.498(10)
Bond angles (°)	
C(2)–O(1)–C(4)	117.2(4)
C(3)–O(2)–C(14)	119.0(4)
C(2)–C(1)–C(3a)	119.2(5)
O(1)–C(2)–C(1)	123.7(5)
O(1)–C(2)–C(3)	116.4(5)
C(1)–C(2)–C(3)	119.8(5)
O(2)–C(3)–C(2)	116.4(5)
O(2)–C(3)–C(1a)	122.7(5)
C(2)–C(3)–C(1a)	120.9(6)
O(1)–C(4)–C(5)	107.8(4)
C(4)–C(5)–C(6)	114.6(4)
C(5)–C(6)–C(7)	113.3(4)
C(6)–C(7)–C(8)	115.1(5)
C(7)–C(8)–C(9)	113.8(5)
O(2)–C(14)–C(15)	107.3(5)
C(14)–C(15)–C(16)	116.5(6)
C(15)–C(16)–C(17)	116.0(6)
Torsion angles (°)	
C(1)–C(2)–C(3)–C(1a)	−0.6(8)
O(1)–C(2)–C(3)–O(2a)	1.6(7)
C(4)–O(1)–C(2)–C(1)	−3.5(7)
C(4)–O(1)–C(2)–C(3)	175.4(4)
C(2)–O(1)–C(4)–C(5)	−179.8(4)
O(1)–C(4)–C(5)–C(6)	64.3(6)
C(4)–C(5)–C(6)–C(7)	176.3(5)
C(14)–O(2)–C(3)–C(1a)	22.2(7)
C(14)–O(2)–C(3)–C(2)	−159.0(5)
C(3)–O(2)–C(14)–C(15)	174.6(5)
O(2)–C(14)–C(15)–C(16)	−57.7(7)
C(14)–C(15)–C(16)–C(17)	178.0(6)

rings is 2.71 Å. As indicated by the large tilt angle and short perpendicular distance no effective π-overlap between successive benzene rings occurs. Compound **3e** is centrosymmetrical and crystallizes in the space group $P\bar{1}$ ($Z = 1$, for general crystal data, Table 3). Salient structural features are reported in Table 9. Compound **3e** possesses a board-like molecular structure [Fig. 7(*a*)]. The benzene ring and the oxygen atoms occupy the same plane; carbon atoms C(4) and C(14) are positioned slightly above the benzene ring [least square plane 0.11 and 0.43 Å, respectively, dihedral angles C(1)–C(2)–O(1)–C(4) = −3.5° and C(14)–O(2)–C(3)–C(1a) = 22.2°]. Although gauche kinks at attachment points align the alkyl chains longitudinally [torsion angles: O(1)–C(4)–C(5)–C(6) = 64.3° and O(2)–C(14)–C(15)–C(16) = −57.7°], the alkoxy chains possess a fully extended antiperiplanar conformation, the two alkoxy chain axes do not run parallel. Nevertheless, their packing leads again to stacking of the central benzene ring along the *a*-axis [Fig. 7(*b*)]. Since the centre-to-centre distance is 4.70 Å (= length *a*-axis) and the tilt angle between the normal on the benzene plane and the *a*-axis amounts 47.9°, the benzene units overlap only moderately. In contrast to **2e**, the perpendicular distance between two successive benzene moieties equals the theoretically possible closest distance of 3.3 Å. Like **2e**, no two-dimensional layered packing of the alkoxy chains is observed.

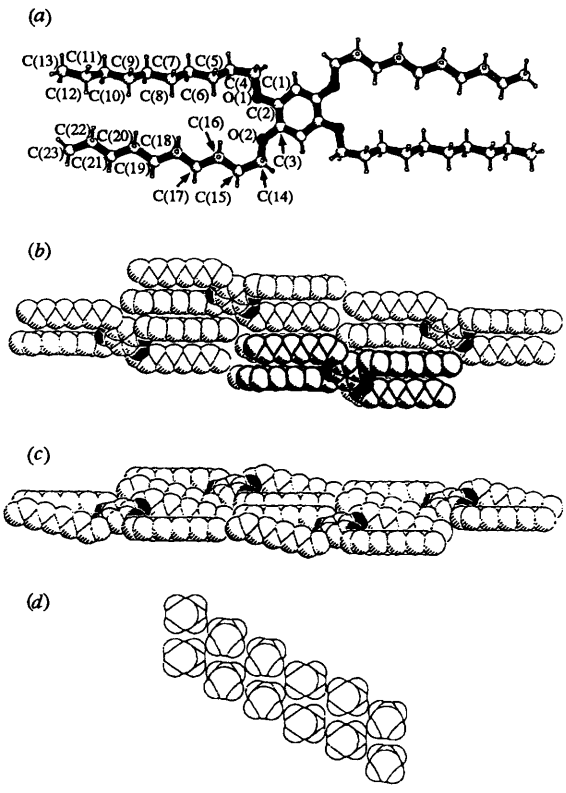

Fig. 7 1,2,4,5-Tetradecyloxybenzene **3e** (*a*) single crystal X-ray structrure, (*b*) top view of alkoxy chain packing; additionally, one molecule in the adjacent layer is depicted bold, (*c*) side view of (*b*), (*d*) cross-section of the alkoxy chain packing showing C(8), C(9), C(18) and C(19)

In the *b* and *c* direction, molecules **3e** are lying only partially side by side, like bricks in a wall [Fig. 7(*b*) and (*c*)]. A cross-section through the alkoxy chain packing at the middle of the alkoxy chains showing C(8), C(9), C(18) and C(19) demonstrates the close packing principle of the chains [Fig. 7(*d*)].

Finally, compounds **1e**, **2e** and **3e** show comparable one-dimensional packing arrangements along their *a*-axis as a result of self-organization of the alkoxy chains. The resulting one-dimensional layers assemble side by side either in two-dimensional layers as proposed for **1e** or interlock like bricks in a wall (**2e** and **3e**).

Summary

We have shown that the intermolecular organization of 1,4-benzoquinone can be improved by substitution with four alkoxy side groups. The $E_{\frac{1}{2}}^{red}(0/-1)$ of the tetraalkoxy-1,4-benzoquinones **1** decreases only moderately (*ca.* −0.15 V), because two *para*-related alkoxy substituents are twisted out-of-plane having only an electron withdrawing inductive effect, while the other two *para*-related alkoxy substituents are coplanar and also give rise to a mesomeric interaction with the 1,4-benzoquinone π-system. Due to this mesomeric effect a merocyanine-type distortion of the 1,4-benzoquinone skeleton occurs. An analysis of the solid state structures reveals that for **1a** short intermolecular C–H···O contacts in combination with reduction of unfavourable dipole–dipole interactions are primarily responsible for the formation of parallel stacked ribbon type structures. One-dimensional stacking along the *a*-axis with a centre-to-centre distance of 4.00 Å indicative of effective π-overlap between 1,4-benzoquinone moieties in successive planes is found. In contrast to **1a**, the close packing principle of alkyl chains determines the solid state packing motif of tetradecyloxy-1,4-benzoquinone **1e**. The single crystal X-ray structures of the structurally related compounds 1,4-diacetoxy-2,3,5,6-tetradecyloxybenzene **2e** and 1,2,4,5-tetra-

decyloxybenzene **3e** support this conclusion. Both **2e** and **3e** possess board-like structures and stack along the *a*-axis due to the close packing of the long alkoxy chains.

Experimental

All reagents were purchased from Janssen Chimica, except for PtO_2 (Aldrich). Diethyl ether was freshly distilled from sodium–benzophenone. Absolute methanol was stored on activated 4 Å molecular sieves. All reactions were carried out under a nitrogen atmosphere, unless indicated otherwise. NMR spectra were recorded on a Bruker AC 300 spectrometer (^{1}H: 300 MHz; ^{13}C: 75 MHz) using the solvent ($CDCl_3$: ^{1}H, δ 7.26; ^{13}C, δ 77.00) as internal standard. *J* values are given in Hz. DRIFT spectra were measured on a Mattson Galaxy Series FTIR 5000 spectrophotometer. Mass spectra were measured with a JEOL JMS-AX505W mass spectrometer (Xe) and reported [matrix] (*m/z*; %, fragment). Melting points were determined on a Mettler FP5/FP51 photo-electric melting point apparatus and are uncorrected. Thermogravimetry analyses were measured using a Perkin-Elmer TGS-2 with an autobalance AR-2. DSC measurements were performed on a Perkin-Elmer DSC 12E in the temperature range between −20 and T_m +20 °C with a heating and cooling rate of 2 °C min^{-1}. Cyclic voltammograms were recorded in acetonitrile and dichloromethane, containing Bu_4PF_6 (10^{-1} mol dm^{-3}) as electrolyte, at a voltage sweep rate of 100 mV s^{-1}. The following three-electrode arrangements were used: (*a*) Pt as working and counter electrode together with a separated Ag/AgCl reference electrode in acetonitrile, containing Bu_4PF_6 (10^{-1} mol dm^{-3}), connected *via* a salt bridge; (*b*) Pt as working and counter electrode together with a separated Ag/AgI reference electrode in dichloromethane, containing Bu_4PF_6 (10^{-1} mol dm^{-3}) and Bu_4PI_6 (10^{-2} mol dm^{-3}), connected *via* a glass frit. Maximum compensation for iR-drop was achieved by utilizing a PAR 273 potentiostat. Reduction potentials are reported against ferrocene as internal standard.[40] Wide angle X-ray diffraction patterns were obtained at ambient temperature using a Delft Instruments Guinier Johansson FR552 camera at a wavelength of 1.5405 Å.

General procedure for the synthesis of 1,2,4,5-tetraalkoxybenzenes 3a–e

2,5-Dihydroxy-1,4-benzoquinone **6** was purified *via* the following procedure. After dissolving **6** (50 g) in boiling dioxane (1.6 dm^3), followed by hot filtration divided over four coarse filters (Selecta folded filters nr 1117.5, Schleicher & Schüll) to remove the insoluble material, the product crystallized upon cooling as its complex with dioxane (yellow plates). After filtration the product was dried for 3 days at 40 °C *in vacuo* to remove the physisorbed dioxane.

A 1 dm^3 three-necked round-bottomed flask was charged with purified 2,5-dihydroxy-1,4-benzoquinone (28 g, 0.20 mol), dimethylformamide (DMF) (500 cm^3) and PtO_2 (0.2 g) as catalyst and was subjected to hydrogenation[41] [P(H_2) 1 atm] with stirring.† After completion of the reaction indicated by the amount of hydrogen gas consumed (4.8 dm^3, 0.20 mol) and decoloration of the reaction mixture, the hydrogen atmosphere was replaced by nitrogen after which potassium carbonate (165 g, 1.20 mol) and the appropriate alkyl bromide (0.802 mol) were added. Subsequently, this reaction mixture was stirred for 96 h at 50 °C. After cooling to room temperature the reaction mixture was poured into water (2 dm^3) followed by extraction with dichloromethane (1 dm^3). The organic layer was separated and the aqueous layer was extracted with dichloromethane (2 × 500 cm^3). The combined organic layers were washed with water (2 × 100 cm^3), dried ($MgSO_4$) and concentrated under reduced pressure. The crude product was crystallized from acetone (1 g in 10 cm^3) at −20 °C.

2,5-Dihydroxy-1,4-benzoquinone. Yield: 36 g (72%) of a red powder, mp 211 °C (lit.,[42] 211 °C); ν_{max}(KBr)/cm^{-1} 3300br, 3100 and 1700–1500br; δ_H([$^2H_6$]DMSO) 8.85 (2 H, br s) and 5.79 (s, 2 H).

1,2,4,5-Tetramethoxybenzene 3a. Yield: 33.97 g (86%) of a white crystalline solid, mp 102.3 °C (lit.,[43] 103 °C); λ_{max}(CH_2Cl_2)/nm (log ε) 296 (3.82) and 232 (4.03); ν_{max}(KBr)/cm^{-1} 3020, 2980, 2860, 1545, 1485, 1455, 1410, 1235 and 1210; δ_H 6.61 (2 H, s) and 3.85 (12 H, s); δ_C 143.61, 100.74 and 57.02.

1,2,4,5-Tetrapropoxybenzene 3b. Yield: 54.12 g (87%) of a white crystalline solid, mp 63.5 °C; λ_{max}(CH_2Cl_2)/nm (log ε) 295 (3.68) and 232 (3.88); ν_{max}(KBr)/cm^{-1} 2960, 2765, 1525, 1470, 1410, 1390, 1235 and 1210; δ_H 6.59 (2 H, s), 3.90 (8 H, t, $^3J_{HH}$ 6.6), 1.79 (8 H, m) and 1.03 (12 H, t, $^3J_{HH}$ 7.4); δ_C 143.70, 105.89, 72.22, 22.88 and 10.53.

1,2,4,5-Tetrahexyloxybenzene 3c. Yield: 89.39 g (93%) of a white crystalline solid, mp 47.8 °C; λ_{max}(hexane)/nm (log ε) 292 (3.79) and 229 (4.03); ν_{max}(KBr)/cm^{-1} 2940, 2850, 1500, 1463, 1410, 1375, 1210 and 1175; δ_H 6.57 (2 H, s), 3.93 (8 H, t, $^3J_{HH}$ 6.6), 1.76 (8 H, m), 1.7–1.3 (24 H, m) and 0.90 (12 H, t, $^3J_{HH}$ 6.7); δ_C 143.54, 105.57, 70.55, 31.58, 29.48, 25.68, 22.57 and 13.97.

1,2,4,5-Tetraoctyloxybenzene 3d. Yield: 113.36 g (96%) of a white crystalline solid, mp 61.8 °C; λ_{max}(hexane)/nm (log ε) 292 (3.78) and 229 (4.02); ν_{max}(KBr)/cm^{-1} 2960, 2920, 2850, 1530, 1465, 1410, 1390, 1222 and 1200; δ_H 6.57 (2 H, s), 3.93 (8 H, t, $^3J_{HH}$ 6.6), 1.76 (8 H, m), 1.5–1.2 (40 H, m) and 0.88 (12 H, t, $^3J_{HH}$ 6.7); δ_C 143.57, 105.62, 70.62, 31.83, 29.57, 29.42, 29.30, 26.06, 22.67 and 14.11.

1,2,4,5-Tetradecyloxybenzene 3e. Yield: 130.63 g (93%) of a white crystalline solid, mp 68.8 °C; λ_{max}(CH_2Cl_2)/nm (log ε) 295 (3.78) and 232 (4.03); ν_{max}/cm^{-1} 2950, 2920, 2840, 1528, 1462, 1410, 1390, 1222 and 1197; δ_H 6.57 (2 H, s), 3.93 (8 H, t, $^3J_{HH}$ 6.6), 1.76 (8 H, m), 1.5–1.2 (56 H, m) and 0.88 (12 H, t, $^3J_{HH}$ 6.7); δ_C 143.67, 105.82, 70.68, 31.92, 29.65, 29.60, 29.47, 29.35, 26.08, 22.68 and 14.09.

General procedure for the synthesis of 1,4-dibromo-2,3,5,6-tetraalkoxybenzenes 4a–e

A 1 dm^3 one-necked round-bottom flask equipped with a condenser was charged with the appropriate 1,2,4,5-tetraalkoxybenzene **3** (0.15 mol) and glacial acetic acid (300 cm^3). A solution of bromine (71.9 g, 0.45 mol) in glacial acetic acid (300 cm^3) was added to the magnetically stirred suspension. Subsequently, the reaction mixture was refluxed for 15 min and stirred for an additional 20 h at room temperature. Afterwards the solvent and excess of bromine were removed under reduced pressure and the residue was crystallized from acetone (1 g in 10 cm^3) at −20 °C. The precipitate was collected by filtration, washed with cold methanol (−20 °C), and dried *in vacuo*.

1,4-Dibromo-2,3,5,6-tetramethoxybenzene 4a. Yield: 33.52 g (63%) of a white crystalline solid (four crystallizations were necessary due to charge-transfer complex formation between **3a** with the excess of bromine), mp 132.9 °C; λ_{max}(CH_2Cl_2)/nm (log ε) 287 (3.26); ν_{max}(KBr)/cm^{-1} 3000, 2980, 2940, 2860, 2810, 1470, 1400, 1387, 1050 and 995; δ_H 3.87 (12 H, s); δ_C 148.02, 112.82 and 61.00; *m/z* (FAB) [glycerol] 358, 356 and 354 (45:85:45, isotope pattern M$^{\bullet+}$).

1,4-Dibromotetrapropoxybenzene 4b. Yield: 55.03 g (78%) of a white crystalline solid, mp 60.0 °C; λ_{max}(CH_2Cl_2)/nm (log ε) 288 (3.25); ν_{max}(KBr)/cm^{-1} 2960, 2940, 2880, 2850, 1470, 1445, 1380 and 1060; δ_H 3.95 (8 H, t, $^3J_{HH}$ 6.7), 1.82 (8 H, m) and 1.05 (12 H, t, $^3J_{HH}$ 7.4); δ_C 147.26, 113.56, 75.58, 23.43 and 10.55; *m/z* (FAB) [*m*-nitrobenzyl alcohol] 470, 468 and 466 (50:100:50, isotope pattern M$^{\bullet+}$).

1,4-Dibromo-2,3,5,6-tetrahexyloxybenzene 4c. Yield: 67.89 g (72%) of a white crystalline solid, mp 52.8; λ_{max}(CH_2Cl_2)/nm (log ε) 288 (3.25); ν_{max}(KBr)/cm^{-1} 2960, 2930, 2860, 1470,

† See footnote on p. 229.

1445, 1380 and 1065; δ_H 3.98 (8 H, t, ^3J 6.7), 1.80 (8 H, m), 1.6–1.3 (24 H, m) and 0.91 (12 H, t, $^3J_{HH}$ 6.7); δ_C 147.29, 113.58, 74.12, 31.66, 30.14, 25.70, 22.62 and 14.03; *m/z* (FAB) [*m*-nitrobenzyl alcohol] 638, 636 and 634 (13:25:13, isotope pattern $M^{\bullet+}$).

1,4-Dibromo-2,3,5,6-tetraoctyloxybenzene 4d. Yield: 90.03 g (80%) of a white crystalline solid, mp 67.7 °C; $\lambda_{max}(CH_2Cl_2)$/nm (log ε) 288 (3.25); ν_{max}(KBr)/cm^{-1} 2960, 2930, 2860, 1470, 1450, 1380, 1065 and 1030; δ_H 3.97 (8 H, t, $^3J_{HH}$ 6.7), 1.79 (8 H, m), 1.5–1.2 (40 H, m) and 0.88 (12 H, t, $^3J_{HH}$ 6.7); δ_C 147.29, 113.59, 74.11, 31.84, 30.18, 29.43, 29.28, 26.05, 22.66 and 14.08; *m/z* (FAB) [*m*-nitrobenzyl alcohol] 750, 748 and 746 (7:15:7, isotope pattern $M^{\bullet+}$).

1,4-Dibromo-2,3,5,6-tetradecyloxybenzene 4e. Yield: 103.32 g (80%) of a white crystalline solid, mp 73.1 °C; $\lambda_{max}(CH_2Cl_2)$/nm (log ε) 288 (3.32); ν_{max}(KBr)/cm^{-1} 2960, 2920, 2850, 1470, 1450, 1420, 1365 and 1030; δ_H 3.98 (8 H, t, $^3J_{HH}$ 6.7), 1.81 (8 H, m), 1.5–1.2 (56 H, m) and 0.90 (12 H, t, $^3J_{HH}$ 6.7); δ_C 147.28, 113.58, 74.11, 31.91, 31.65, 30.18, 29.91, 29.63, 29.60, 29.48, 29.34, 22.69 and 14.11; *m/z* (FAB) [*m*-nitrobenzyl alcohol] 862, 860 and 858 (5:10:5, isotope pattern $M^{\bullet+}$).

2,3,5,6-Tetraalkoxybenzene-1,4-diboronic acids 5b–e

Compounds **5b–e** were obtained by crystallization of the crude diboronic acid from either hexane (**5b,e**) or dichloromethane (**5c,d**) (*cf.* general procedure for the synthesis of 2,3,5,6-tetraalkoxy-1,4-benzoquinones). As expected, the ^{13}C NMR spectra of **5b–e** determined at room temperature lacked the signal for the boron-bonded carbon atom due to quadrupolar relaxation phenomena.[44] Since the latter are temperature dependent, ^{13}C NMR spectroscopy at reduced temperature will lead to a sharp signal due loss of boron–carbon coupling. At −40 °C the ^{13}C NMR spectra of **5e** ($CDCl_3$, relaxation delay of 5 s) showed the signal for the boron-bonded carbon atom at δ 120.4.

2,3,5,6-Tetrapropoxybenzene-1,4-diboronic acid 5b. Yield 2.99 g (30%) of a white solid; $\lambda_{max}(CH_2Cl_2)$/nm (log ε) 314 (3.6); ν_{max}(KBr)/cm^{-1} 3500br, 2960, 2940, 2880, 1430, 1370, 1345 and 1070; δ_H 7.41 (4 H, s, disappeared upon addition of ^2H_2O), 4.00 (8 H, t, $^3J_{HH}$ 7.1), 1.83 (8 H, m) and 1.03 (12 H, t, $^3J_{HH}$ 7.4); δ_C 152.65, 99.44, 76.59, 23.35 and 10.18; *m/z* (FAB) [*m*-nitrobenzyl alcohol] 938 [55, M^+ + 4 × (*m*-nitrobenzyl alcohol − H_2O)] and 803 [55, M^+ + 3 × (*m*-nitrobenzyl alcohol − H_2O)].

2,3,5,6-Tetrahexyloxybenzene-1,4-diboronic acid 5c. Yield 5.06 g (72%) of a white solid; $\lambda_{max}(CH_2Cl_2)$/nm (log ε) 314 (3.6); ν_{max}(KBr)/cm^{-1} 3500vbr, 2960, 2930, 2880, 2860, 1430, 1400–1300br and 1050br; δ_H 7.42 (4 H, s, disappeared upon addition of ^2H_2O), 4.02 (8 H, t, $^3J_{HH}$ 7.1), 1.80 (8 H, m), 1.50–1.25 (24 H, m) and 0.90 (12 H, t, $^3J_{HH}$ 6.9); δ_C 152.72, 99.44, 75.31, 31.56, 30.10, 25.45, 22.51 and 13.94; *m/z* (FAB) [*m*-nitrobenzyl alcohol] 1106 [10, M^+ + 4 × (*m*-nitrobenzyl alcohol − H_2O)] and 803 [2, M^+ + 3 × (*m*-nitrobenzyl alcohol − H_2O)].

2,3,5,6-Tetraoctyloxybenzene-1,4-diboronic acid 5d. Yield 7.49 g (44%) of a white solid; $\lambda_{max}(CH_2Cl_2)$/nm (log ε) 314 (3.7); ν_{max}(KBr)/cm^{-1} 3400vbr, 2960, 2930, 2880, 2860, 1430, 1400–1300br and 1050br; δ_H 7.43 (4 H, s, disappeared upon addition of ^2H_2O), 4.01 (8 H, t, $^3J_{HH}$ 7.1), 1.80 (8 H, m) 1.50–1.25 (40 H, m) and 0.89 (12 H, t, $^3J_{HH}$ 6.9); δ_C 152.71, 99.44, 75.31, 31.74, 30.15, 29.37, 29.16, 25.80, 22.61 and 14.04; *m/z* (FAB) [*m*-nitrobenzyl alcohol] 1218 [2, M^+ + 4 × (*m*-nitrobenzyl alcohol − H_2O)].

2,3,5,6-Tetradecyloxybenzene-1,4-diboronic acid 5e. Yield 12.04 g (61%) of a white solid; $\lambda_{max}(CH_2Cl_2)$/nm (log ε) 314 (3.7); ν_{max}(KBr)/cm^{-1} 3400vbr, 2960, 2930, 2880, 2860, 1430, 1400–1300br and 1050br; δ_H 7.42 (4 H, s, disappeared upon addition of ^2H_2O), 4.01 (8 H, t, $^3J_{HH}$ 7.1), 1.80 (8 H, m), 1.50–1.25 (56 H, m) and 0.88 (12 H, t, $^3J_{HH}$ 6.9); δ_C 152.67, 99.44, 75.01, 31.85, 30.08, 29.59, 29.57, 29.41, 25.70, 22.71 and 14.27; *m/z* (FAB) [*m*-nitrobenzyl alcohol] 1330 [2, M^+ + 4 × (*m*-nitrobenzyl alcohol − H_2O)].

General procedure for the syntheses of 2,3,5,6-tetraalkoxy-1,4-benzoquinones 1b–e

A 500 cm^3 one-necked round-bottom flask equipped with a septum piece combined with a nitrogen inlet was charged with the appropriate 1,4-dibromo-2,3,5,6-tetraalkoxybenzene **2** (25 mmol) and diethyl ether (125 cm^3). A solution of butyllithium in hexane (47 cm^3, 55 mmol; 1.16 mol dm^{-3}) was added to the magnetically stirred solution. After 15 min trimethyl borate (10 cm^3, 95 mmol) was added to the solution and stirring was continued for 15 min giving a highly viscous, gel-like reaction mixture. Upon addition of absolute methanol (125 cm^3) a clear solution was obtained. After reduction of the volume under reduced pressure at ambient temperature, the residue was dissolved in benzene (250 cm^3). The reaction mixture was stirred three times with water (150 cm^3) for 90 min giving the crude diboronic acid derivatives **5b–e**. [The latter procedure is necessary to warrant quantitative hydrolysis of the trimethylborate ester (^1H NMR).]‡ For the conversion of **5** into the desired 1,4-benzoquinones **1** the benzene layer was stirred twice for 6 and 18 h, respectively, with a hydrogen peroxide solution (75 cm^3, 35 wt% in water) to which a solution of Aliquat 336 in benzene [4.5 cm^3 (1 g Aliquat 336:100 cm^3 benzene)] and glacial acetic acid (0.15 cm^3) were added. After the second treatment the reaction mixture contained both the 1,4-benzoquinone **1** and its related hydroquinone (^1H NMR). The latter were further oxidized by addition of potassium carbonate (9.0 g, aqueous layer pH 8) followed by additional stirring for 4 days. Subsequently, the benzene layer was separated, washed with water (3 × 50 cm^3), dried ($MgSO_4$) and the solvent was evaporated under reduced pressure. The product was purified by column chromatography (basic aluminum oxide; eluent: ethyl acetate–hexane 1:1).

2,3,5,6-Tetrapropoxy-1,4-benzoquinone 1b. Yield 4.58 g (54%) of a red oil; $\lambda_{max}(CH_2Cl_2)$/nm (log ε) 410 (2.51) and 303 (4.12); ν_{max}(NaCl)/cm^{-1} 2960, 2925, 2870, 1655, 1595 and 1265; δ_H 4.06 (8 H, t, $^3J_{HH}$ 6.7), 1.70 (8 H, m) and 0.94 (12 H, t, $^3J_{HH}$ 7.4); δ_C 180.86, 142.86, 75.32, 23.20 and 10.05; *m/z* (FAB) [glycerol] 342 [50, $(M + 2H)^+$], 341 [97, $(M + H)^+$], 340 (75, $M^{\bullet+}$) and 173 {100, $[M - (4 \times C_3H_6) + H]^+$}.

2,3,5,6-Tetrahexyloxy-1,4-benzoquinone 1c. Yield 11.27 g (88%) of a red oil; $\lambda_{max}(CH_2Cl_2)$/nm (log ε) 410 (2.52) and 303 (4.12); ν_{max}(NaCl)/cm^{-1} 2950, 2920, 2870, 1655, 1595 and 1260; δ_H 4.13 (8 H, t, $^3J_{HH}$ 6.7) 1.72 (8 H, m), 1.4–1.2 (24 H, m) and 0.89 (12 H, t, $^3J_{HH}$ 6.7); δ_C 180.89, 142.97, 73.91, 31.75, 30.01, 29.25, 25.67, 22.58 and 13.96; *m/z* (FAB) [glycerol] 510 [25, $(M + 2H)^+$], 509 [35, $(M + H)^+$], 508 (40, $M^{\bullet+}$) and 173 {100, $[M - (4 \times C_6H_{12}) + H]^+$}.

2,3,5,6-Tetraoctyloxy-1,4-benzoquinone 1d. Yield 12.52 g (81%) of a red oil; $\lambda_{max}(CH_2Cl_2)$/nm (log ε) 410 (2.50) and 303 (4.12); ν_{max}(NaCl)/cm^{-1} 2955, 2925, 2860, 1660, 1595 and 1265; δ_H 4.13 (8 H, t, $^3J_{HH}$ 6.7), 1.72 (8 H, m), 1.4–1.2 (40 H, m) and 0.89 (12 H, t, $^3J_{HH}$ 6.7); δ_C 180.77, 142.72, 73.71, 31.60, 29.84, 29.10, 29.02, 25.51, 22.43 and 13.82; *m/z* (FAB) [glycerol] 622 [18, $(M + 2H)^+$], 621 [22, $(M + H)^+$], 620 (23, $M^{\bullet+}$) and 173 {100, $[M - (4 \times C_8H_{16}) + H]^+$}.

2,3,5,6-Tetradecyloxy-1,4-benzoquinone 1e. Yield 17.06 g (93%) of a red crystalline solid; $\lambda_{max}(CH_2Cl_2)$/nm (log ε) 410 (2.52) and 303 (4.12); ν_{max}(KBr)/cm^{-1} 2960, 2925, 2840, 1655, 1595 and 1260; δ_H 4.13 (8 H, t, $^3J_{HH}$ 6.7), 1.72 (8 H, m), 1.4–1.2 (56 H, m) and 0.88 (12 H, t, $^3J_{HH}$ 6.7); δ_C 180.99, 142.97, 74.00, 31.86, 30.02, 29.52, 29.31, 29.17, 25.95, 22.64 and 14.05; *m/z* (FAB) [glycerol] 734 [20, $(M + 2H)^+$], 733 [17, (M +

‡ See footnote on p. 230.

H)$^{\bullet+}$], 732 (15, $M^{\bullet+}$) and 173 {100, [M − (4 × $C_{10}H_{20}$) + H]$^+$}.

2,3,5,6-Tetramethoxy-1,4-benzoquinone 1a

A 1 dm^3 three-necked round-bottom flask equipped with a septum and condenser containing a nitrogen outlet, was charged with chloranil (9.84 g, 0.16 mol) and absolute methanol (200 cm^3). To the refluxing solution a sodium methoxide solution [3.68 g (0.16 mol) sodium in absolute methanol (200 cm^3)] was added *via* syringe. The solution turned dark and was refluxed for 30 min after which it was immediately filtered. Upon slowly cooling the filtrate to 4 °C **1a** crystallized as a red solid (5.74 g, 63%), T_m (onset DSC peak) = 127.0 °C (lit.,[12] 135 °C); $\lambda_{max}(CH_2Cl_2)$/nm (log ε) 410 (2.48) and 303 (4.11); ν_{max}(KBr)/cm^{-1} 3010, 2950, 2840, 1660, 1600, 1460, 1440, 1370, 1070 and 1060; δ_H 3.99 (12 H, s); δ_C 180.36, 142.72 and 61.26; *m/z* (FAB) [glycerol] 230 [33, $(M + 2H)^+$], 229 [100, $(M + H)^+$] and 228 (45, $M^{\bullet+}$).

1,4-Diacetoxy-2,3,5,6-tetraalkoxybenzenes 2a,e

Compounds **2a** and **e** were prepared according to a reported procedure.[15]

1,4-Diacetoxy-2,3,5,6-tetramethoxybenzene 2a. Compound **2a** was crystallized from acetone. Yield 1.23 g (78%) of a white crystalline solid, mp 131.4 °C; $\lambda_{max}(CH_2Cl_2)$/nm (log ε) 277 (3.11) and 229 (3.84); ν_{max}(KBr)/cm^{-1} 3020, 2960, 1790, 1485, 1190 and 1180; δ_H 3.82 (12 H, s) and 2.35 (6 H, s); δ_C 168.66, 142.08, 135.75, 61.12 and 20.34; GC–MS: 314 (20, $M^{\bullet+}$) and 230 {100, [M − (2 × CH_2CO)]$^+$}.

1,4-Diacetoxy-2,3,5,6-tetradecyloxybenzene 2e. Compound **2e** was crystallized from acetone–methanol (1 : 1). Yield 1.78 g (80%) of a white crystalline solid, mp 82.7 °C; $\lambda_{max}(CH_2Cl_2)$/nm (log ε) 276 (3.54) and 229 (4.26); ν_{max}(KBr)/cm^{-1} 2920, 1840, 1770, 1140 and 1190; δ_H 3.93 (8 H, t, $^3J_{HH}$ 6.5), 2.31 (6 H, s), 1.67 (8 H, m), 1.4–1.1 (56 H, m) and 0.88 (12 H, s); δ_C 168.43, 141.53, 135.75, 74.10, 31.90, 30.26, 29.66, 29.60, 29.48, 29.34, 26.04, 22.68, 20.44 and 14.10; *m/z* (FAB) [glycerol] 818 (15, $M^{\bullet+}$), 174 {100, [M − (2 × CH_2CO) − (4 × $C_{10}H_{20}$)]$^+$} and 173 (100).

Theoretical calculations

For the theoretical calculations on 1,4-benzoquinones and acroleins the semi-empirical quantum mechanical Hamiltonian AM1[45] (MOPAC 6.0)[46] was used.¶ The input geometries were generated using PCMODEL[47] and pre-optimized with the MMX force field. Subsequently, all structures were optimized without any geometrical constraints using the PRECISE option (MOPAC). Minima were characterized by calculating their Hessians [FORCE and LARGE option (MOPAC)].

X-Ray crystal structure determination of 1a, 2a, 2e and 3e

Crystals suitable for X-ray diffraction were glued to a Lindemann-glass capillary and transferred to an Enraf-Nonius CAD4-T diffractometer on rotating anode (**1a** and **2e**) or to an Enraf-Nonius CAD4-F diffractometer on sealed tube (**2a** and **3e**). Accurate unit-cell parameters and an orientation matrix were determined by least-squares refinement of the setting angles of 25 well-centred reflections (SET4). Reduced-cell calculations did not indicate higher lattice symmetry[48] for any of the studied compounds. Crystal data and details on data collection and refinement are collected in Table 3. Data were corrected for Lp effects and, if neccessary, for the observed linear decay of the reflections. The standard deviations of the intensities as obtained by counting statistics were increased according to an analysis of the excess variance of the reflections: $\sigma^2(I) = \sigma^2_{CS}(I) + (pI)^2$ with p = 0.01, 0.03 and 0.009 for **2a**, **2e** and **3e**, respectively.[49] Empirical absorption and extinction correction were applied for compound **3e** (DIFABS);[50] no absorption correction was applied for the other compounds. The F_c values of **2a** and **2e** were corrected for secondary extinction by refinement of an empirical isotropic parameter: $F'_c = F_c[1 - xF^2_c/\sin\ \theta]$ with $x = 1.12(9) \times 10^{-6}$ and $2.4(1) \times 10^{-7}$ for **2a** and **2e**, respectively. All structures were solved by direct methods (SHELXS 86).[51] Compounds **2a**, **2e** and **3e** were refined on F by full-matrix least-squares techniques (SHELXL 76).[52] Compound **1a**, however, was refined on F^2, also using full-matrix least-squares techniques (SHELXL 93);[53] no observance criterium was applied during refinement. Hydrogen atoms of **2a** and **3e** were included in the refinement on calculated positions (C–H = 0.98 Å), riding on their carrier atoms. The methyl hydrogen atoms of **2a** were refined as a rigid group. The hydrogen atoms of **1a** and **2e** were located on a difference Fourier map and subsequently included in the refinement. The non-hydrogen atoms of all structures were refined with anisotropic thermal parameters. Hydrogen atoms of **2a** were refined with one overall isotropic thermal parameter amouting to 0.133(4) Å^2. The hydrogen atoms of **3e** were refined with two overall isotropic thermal parameters with values of 0.179(11) and 0.082(4) Å^2 for the hydrogen atoms of the methyl group and the other hydrogen atoms, respectively. The hydrogen atoms of **1a** and **2e** were included in the refinement with individual isotropic thermal parameters. Neutral atom scattering factors and anomalous dispersion corrections were taken from the *International Tables for Crystallography* for **1a**.[54] The other compounds were refined using neutral atom scattering factor taken from Cromer and Mann[55] amplified with anomalous dispersion corrections from Cromer and Liberman.[56] Geometrical calculations and illustrations were performed with PLATON;[57] all calculations were performed on a DEC stations 5000 cluster. Further details of the structure determinations, including a complete list of atomic coordinates, bond lengths and angles and thermal parameters have been deposited and are available from the Cambridge Crystallographic Data Centre.‖

Acknowledgements

This investigation was supported in part by the Ministry of Economic Affairs of the Netherlands (IOP) with financial aid (E. M. D. K.) and by the Netherlands Foundation of Chemical Research (SON) with financial aid (A. L. S., N. V.) from the Netherlands Organization for Scientific Research (NWO).

¶ See footnote on p. 231.

‖ For details of the CCDC deposition scheme see Instructions for Authors, *J. Chem. Soc., Perkin Trans. 2*, 1996, issue 1.

References

1 J. Q. Chambers, *The Chemistry of the Quinonoid Compounds*, ed. S. Patai, Wiley, London, 1974, p. 737.
2 S. Hünig, *Pure Appl. Chem.*, 1990, **62**, 395.
3 T. J. Meyer, *Acc. Chem. Res.*, 1989, **101**, 693 and references cited therein.
4 J. B. Torrance, J. J. Mayerle, V. Y. Lee and K. Bechgard, *J. Am. Chem. Soc.*, 1979, **101**, 4747; M. N. Vyayashree and S. V. Subramayam, *Macromolecules*, 1992, **25**, 2986; E. M. D. Keegstra, P. G. Schouten, A. Schouten, H. Kooijman, A. L. Spek, M. P. de Haas, J. W. Zwikker, J. M. Warman and L. W. Jenneskens, *Recl. Trav. Chim. Pays-Bas*, 1993, **112**, 423.
5 E. E. Ergozhin, B. A. Mukhitdinova, R. Kh. Bakirova, O. K. Stefanova and N. V. Rozhdestvenskaya, *Reactive Polymers*, Elsevier, Amsterdam, 1992, vol. 16, p. 321.
6 T. A. Reddy, D. Macaione and S. Erhan, *J. Polym. Sci., Part A: Polym. Chem.*, 1994, **32**, 1977 and references cited therein.
7 J. Fabian and R. Zahradnik, *Angew. Chem.*, 1989, **101**, 693; H.-W. Schmidt, *Angew. Chem. Adv. Mater., Int. Ed. Engl.*, 1989, **101**, 964; K. Takazuko, T. Suzuki, K. Akiyama, Y. Ikegami and Y. Fukazawa, *J. Am. Chem. Soc.*, 1991, **113**, 4576 and references cited therein.
8 J. A. Zerkowski, C. T. Seto, D. A. Wierda and G. M. Whitesides, *J. Am. Chem. Soc.*, 1990, **112**, 9025; J. S. Lindsey, *New J. Chem.*,

1991, **15**, 153; P. Baxter, J.-M. Lehn, A. DeCain and J. Fischer, *Angew. Chem., Int. Ed. Engl.*, 1993, **32**, 69.
9 J. Bernstein, M. D. Cohen and L. Leiserowitz, *The Chemistry of the Quinonoid Compounds*, ed. S. Patai, Wiley, London, 1974, p. 37 and references cited therein.
10 G. R. Desiraju, *Crystal Engineering: The Design of Organic Solids*, Elsevier, New York, 1989 and references cited therein; T. J. Marks, *Angew. Chem., Int. Ed. Engl.*, 1990, **29**, 857; S. Hünig and P. Erk, *Adv. Mater.*, 1991, **3**, 225.
11 V. Ramamurthy and K. Venkatesan, *Chem. Rev.*, 1987, **87**, 433; N. M. Peachey and C. J. Eckhart, *J. Am. Chem. Soc.*, 1993, **115**, 3519.
12 C. Tanford, *Science*, 1978, **200**, 1012; A. Ulman and R. P. Scaringe, *Langmuir*, 1992, **8**, 894 and references cited therein; F. Garnier, A. Yassar, R. Hajlaoui, G. Horowitz, F. Deloffre, B. Servet, S. Ries and P. Alnot, *J. Am. Chem. Soc.*, 1993, **115**, 8716 and references cited therein.
13 H. Junek, B. Unterweger and R. Peltzman, *Z. Naturforsch., Teil B*, 1978, **33**, 1201.
14 H. Ringsdorf and P. Tschirner, *Makromol. Chem.*, 1978, **188**, 1431.
15 A. Vogel, *Textbook of Practical Organic Chemistry*, Longmans, London, 4th edn., 1978, p. 1115.
16 J. Heinze, *Angew. Chem.*, 1984, **96**, 823.
17 A. Aumüller and S. Hünig, *Liebigs Ann. Chem.*, 1986, 165.
18 R. C. Prince, P. L. Dutton and J. M. Bruce, *FEBS Lett.*, 1983, **160**, 273.
19 S. Berger and A. Rieker, *The Chemistry of the Quinonoid Compounds*, ed. S. Patai, Wiley, London, 1974, p. 186.
20 W. Flaig and J.-C. Salfeld, *Anal. Chem.*, 1959, 215.
21 E. M. D. Keegstra, A. L. Spek, J. W. Zwikker and L. W. Jenneskens, *J. Chem. Soc., Chem. Commun.*, 1994, 1633.
22 Z. Shi, T. Enoki, K. Imaeda, K. Seki, P. Wu, H. Inokuchi and G. Satio, *J. Phys. Chem.*, 1988, **92**, 5044.
23 D. G. Anderson, J. C. Smith and R. J. Rallings, *J. Chem. Soc.*, 1953, 443.
24 A. R. Ubbelhode, *The Molten State of Matter, Melting and Crystal Structure*, Wiley, Chichester, 1978, ch. 7, p. 154.
25 M. G. Broadhurst, *J. Res. Natl. Bur. Stand., Sect. A*, 1962, **66**, 241; M. Maroncelli, S. P. Qi, H. L. Straus and R. G. Snyder, *J. Am. Chem. Soc.*, 1982, **104**, 6237.
26 A. I. Kitaigorodsky, *Molecular Crystals and Molecules*, Academic Press, New York, 1973, 48.
27 A. Bondi, *J. Phys. Chem.*, 1964, **68**, 441.
28 C. Reichardt, *Solvents and Solvent Effects in Organic Chemistry*, VCH, Weinheim, 2nd edn., 1988, p. 285 and references cited therein.
29 K. Mislow, *Introduction to Stereochemistry*, Benjamin/Cummings, 1965.
30 S. Kulpe, D. Leopold and S. Dähne, *Angew. Chem.*, 1966, **78**, 693; S. J. Rettig and J. Trotter, *Can. J. Chem.*, 1974, **53**, 777.
31 H. Bock, K. Ruppert, C. Näther, Z. Havlas, H.-F. Herrmann, C. Arad, I. Göbel, A. John, J. Meuret, S. Nick, A. Rauschenbach, W. Seitz, T. Vaupel and B. Solouki, *Angew. Chem., Int. Ed. Engl.*, 1992, **31**, 550.
32 M. J. S. Dewar and W. Thiel, *J. Am. Chem. Soc.*, 1977, **99**, 4907.
33 J. J. P. Stewart, *J. Comp. Chem.*, 1989, **10**, 221.
34 T. Clark, *A Handbook of Computational Chemistry*, Wiley, New York, 1985.
35 E. M. D. Keegstra, V. Van der Mieden, J. W. Zwikker, L. W. Jenneskens, A. Schouten, H. Kooijman, N. Veldkamp and A. L. Spek, *Chem. Mater.*, submitted.
36 G. A. Jeffrey, H. Maluszynska and J. Mitra, *Int. J. Biol. Macromol.*, 1985, **7**, 336; G. R. Desiraju, *Acc. Chem. Res.*, 1991, **24**, 290 and references cited therein.
37 Cambridge Crystallographic Data Base; F. Bolhuis and C. Th. Kiers, *Acta Crystallogr., Sect. B*, 1978, **34**, 1015.
38 Y. Shnidman, A. Ulman and J. E. Eilers, *Langmuir*, 1993, **9**, 1071.
39 K. von Deuten and G. Klar, *Cryst. Struct. Commun.*, 1979, **8**, 1017.
40 R. R. Gagné, C. A. Koval and G. C. Lisenky, *Inorg. Chem.*, 1980, **19**, 2855.
41 S. A. R. Dewaele, USP 3 780 114/1973.
42 *CRC Handbook of Chemistry and Physics*, ed. R. C. Weast, 61st edn., CRC, Boca Raton, 1980.
43 H. G. H. Erdtman, *Chem. Abstr.*, 1934, **28**, 1337.
44 B. Wrackmeyer, *Prog. Nucl. Magn. Reson. Spectrosc.*, 1979, **12**, 227; B. R. Gragg, W. J. Layton and K. Niedenzu, *J. Organomet. Chem.*, 1977, **132**, 29.
45 M. J. S. Dewar, E. G. Zoebisch, E. F. Healey and J. J. P. Stewart, *J. Am. Chem. Soc.*, 1985, **107**, 3902.
46 J. J. P. Stewart, *Quantum Chemistry Program Exchange*, QCPE 504, Bloomington, IN, USA, 1990.
47 PCMODEL (MMX force field): Serena Software, Bloomington, IN, USA, 1990.
48 A. L. Spek, *J. Appl. Crystallogr.*, 1988, **21**, 578.
49 L. E. McCandlish, G. H. Stout and L. C. Andrews, *Acta Crystallogr., Sect. A*, 1975, **31**, 245.
50 N. Walker and D. Stuart, *Acta Crystallogr., Sect. A*, 1983, **39**, 158.
51 G. M. Sheldrick, SHELXS 86 Program for crystal structure determination, University of Göttingen, Germany, 1986.
52 G. M. Sheldrick, SHELX 76 Program for crystal structure determination, University of Göttingen, Germany, 1976.
53 G. M. Sheldrick, SHELXL 93 Program for crystal structure determination, University of Göttingen, Germany, 1992.
54 *International Tables for Crystallography*, ed. A. J. C. Wilson, vol. C, 1992, Kluwer, Dordrecht, 1992, vol. 2.
55 D. T. Cromer and J. B. Mann, *Acta Crystallogr., Sect. A*, 1968, **24**, 321.
56 D. T. Cromel and D. Liberman, *J. Chem. Phys.*, 1970, **53**, 1891.
57 A. L. Spek, *Acta Crystallogr., Sect. A*, 1990, **46**, C34.

Paper 5/03756E
Received 12*th June* 1995
Accepted 18*th August* 1995